

Global fixed point potential approach to frustrated antiferromagnets

Shunsuke Yabunaka¹ and Bertrand Delamotte²

¹*Advanced Science Research Center,*

Japan Atomic Energy Agency, Tokai, 319-1195, Japan

²*Sorbonne Université, CNRS, Laboratoire de Physique Théorique
de la Matière Condensée, LPTMC, F-75005 Paris, France*

(Dated: January 9, 2025)

Abstract

We revisit the critical behavior of classical frustrated systems using the nonperturbative renormalization group (NPRG) equation. Our study is performed within the local potential approximation of this equation to which is added the flow of the field renormalization. Our flow equations are functional to avoid possible artifacts coming from the field expansion of the fixed point potential which consists in keeping only a limited number of coupling constants. We explain in detail our numerical implementation, its advantages and the difficulties encountered in the vicinity of $d = 2$. For N -component spins, the function $N_c(d)$ separating the regions of first and second order transitions in the (d, N) plane is computed for d between 4 and 2.3. Our results confirm what was previously found with cruder approximations of the NPRG equation and contradict both the fixed dimension perturbative approach and some of the results obtained within the conformal bootstrap approach.

PACS numbers: 75.10.Hk, 05.10.Cc, 12.38.Lg

I. INTRODUCTION

The critical behavior of antiferromagnetic frustrated systems is still a debated question more than forty years after the first studies of these systems [1, 2]. The key difference between frustrated and nonfrustrated systems is that the order parameter is a vector in the nonfrustrated case and a matrix in the other cases. When frustration originates from the geometry of the system as in Stacked Triangular Antiferromagnets (STA), the symmetry of the Hamiltonian is $O(N) \otimes O(2)$ for N -component spins and the order parameter is a rectangular $N \times 2$ matrix [3]. Depending on N and the dimension d of space, the nature of the phase transition changes, being first order for low values of N and dimensions d close to four and second order otherwise. One of the key questions is thus the determination of the line $N_c(d)$ separating the first and second order regions in the (d, N) plane. It turns out that the value of $N_c(d = 3)$ is certainly close to 3 and its precise determination is crucial to know whether the transition is first or second order for the systems realized in nature, that is, for $N = 2$ and 3. Numerical simulations of several frustrated antiferromagnets such as XY and Heisenberg STA have been showing that the transition is first order for these systems [4–7]. However a recent simulation of Heisenberg STA with a very large lattice size found second order transition corresponding to a focus fixed point (FP) [8]. Depending on the theoretical approach considered, the determination of $N_c(d)$ varies much when $d \lesssim 3.3$ and, as a result, it is not yet settled whether all $O(N) \otimes O(2)$ symmetric systems undergo first order phase transitions in $d = 3$ for $N \leq 3$. The two-dimensional physics of the XY and Heisenberg systems is also debated because the relevance of topological defects is not yet understood, in particular the possibility that they trigger a phase transition at finite temperature [9–14].

The different renormalization group approaches tackling with the problem of the calculation of $N_c(d)$ can be roughly divided into two classes: the perturbative and the nonperturbative renormalization group (NPRG) calculations. The class of perturbative calculations can be again divided into several different subclasses depending on whether they are performed directly in $d = 3$ (at six loops) [15–17] or in an ϵ - or pseudo- ϵ -expansion (respectively at six and five loops)[18]. In the latter case, the value of $N_c(d = 3)$ is systematically found larger than 3 (of order 6) as it is also the case for the NPRG calculations that find $N_c(d = 3) \simeq 5.1$ [1, 19–22]. On the contrary, the perturbative calculation performed directly in $d = 3$ at six loops yields a fixed point for $N = 2$ and 3 and thus predicts that several

$O(N) \otimes O(2)$ symmetric systems should undergo a second order phase transition.

Recently, a completely different method based on the conformal bootstrap has been used to study matrix models in $d = 3$ and in particular the $O(N) \otimes O(2)$ frustrated systems [23, 24, 26, 27]. This approach has the advantage of being unbiased by convergence problems since it is not based on series expansions, contrary to RG methods and, when applied to the ferromagnetic $O(N)$ models, it leads to a very accurate determination of the critical exponents, at least when it is truncated at large orders [28, 29]. However for the frustrated systems, the situation is less clear. An early conformal bootstrap study conjectured the existence of a critical FP for $N = 2$ and 3 in $d = 3$, based on kinks of rigorous bounds on scaling dimensions. The predicted critical exponents are in good agreement with those for the focus type of FPs found with the perturbative fixed dimensional approach [23, 24]. However, by construction, the conformal bootstrap cannot find a fixed point with imaginary exponents because this contradicts reflection positivity. It is pointed out in Section 4 of [27] that interpreting a kink as an indication of the existence of a critical FP may not be valid in general. In a recent refined conformal bootstrap study, rigorous bounds are derived to isolate allowed regions in the space of scaling dimensions and it is shown that a lower bound for $N_c(d)$ for systems satisfying reflection positivity is $N_c(d = 3) > 3.78$ [27].

As for the NPRG approach, that we re-examine here, the situation is the following. Either the conclusions drawn from its results are correct and then both the fixed dimension perturbative RG approach and some of the conformal bootstrap studies [23, 24] are wrong or, conversely, it is wrong (together with the ϵ -expansion approaches) and this implies that the approximations used so far are too drastic to reproduce the correct physics. In both cases, something very unusual is at work because the methodologies that have been used in these studies lead in many cases to correct and accurate results, see for instance [25].

The NPRG is based on an exact RG equation that requires approximations to be solved. The approximations used so far to tackle with frustrated systems consists in performing a derivative expansion [30] and a field expansion of the Gibbs free energy [1, 21, 22]. The rationale behind this choice is (i) that the critical behavior of thermodynamic quantities such as the specific heat or the susceptibility for instance are dominated by long wavelength fluctuations which justifies expanding the correlation functions in their momenta (derivative expansion) and (ii) that the impact of the n -point functions with n large on the RG flow of the zero or two-point functions should be small (field-expansion). It is the aim of this

article to eliminate one source of inaccuracy of the NPRG approach, the field expansion, which is known to be inaccurate in low dimensions even for simple models such as the ferromagnetic $O(N)$ models [1]. The price to pay to get rid of this approximation is to work functionally, that is, to follow the RG flow of functions of the fields instead of a limited number of coupling constants. In the case of nonfrustrated systems, this is relatively simple since the $O(N)$ symmetry implies that all functions involved in the RG flows depend on the fields only through the unique $O(N)$ -invariant: $\rho = \vec{\phi}^2$. For frustrated systems, there exists two $O(N) \otimes O(2)$ invariants and the resulting flow equations are partial differential equations that are rather involved to solve numerically. We show in this article how to simplify the numerical problem and point out why the numerical difficulties are so great in low dimensions that our method does no longer work when approaching $d = 2$. We provide the results thus obtained for the curve $N_c(d)$ between $d = 4$ and $d = 2.3$.

We note that in previous NPRG studies involving a field expansion of the potential, it was not possible to study the curve $N_c(d)$ below $d = 3$ in a reliable manner. One of the expected scenarios to allow for the existence of a FP that drives a second order transition in $d = 3$ and $N = 3$ is that $N_c(d)$ does not decrease monotonously but has a turn around point around $d = 3$, see for instance [27]. In this scenario, the curve $N_c(d)$ is continuous but has a S-shape, that is, the first-order region is re-entrant around $d = 3$ and the function $N_c(d)$ is multi-valued in $d = 3$: when N is large, the transition is second-order, becomes first-order for smaller values of N , typically $N < 6$, and becomes second-order again for even smaller values of N , in particular $N = 2$ and 3. Therefore, it is interesting for physics in $d = 3$ to study the part of the curve $N_c(d)$ below $d = 3$ to find out whether or not such a turn around point exists or the curve is monotonous down to $d = 2$. Our results confirm what was previously found within a NPRG approximation involving a field expansion of the potential and the ϵ -approaches and thus contradict both the fixed-dimension perturbative approach and the results obtained with the conformal bootstrap in [23, 24].

II. THE MODEL

As the archetype of frustrated spin systems, we employ the Stacked Triangular Antiferromagnets (STA). This system is composed of two-dimensional triangular lattices that are piled-up in the third direction. At each lattice site i , is defined a N -component vector \mathbf{S}_i of

modulus 1. The Hamiltonian of this system is given by

$$H = J \sum_{\langle ij \rangle} \mathbf{S}_i \cdot \mathbf{S}_j. \quad (1)$$

The sum $\langle ij \rangle$ runs on all pairs of nearest neighbor spins and $J > 0$.

The long distance effective theory for the STA has been derived by Yosefin and Domany[3]. The order parameter consists of the $N \times 2$ matrix $\Phi = (\phi_1, \phi_2)$ that satisfies

$$\phi_i \cdot \phi_j = \delta_{ij} \quad (2)$$

for $i, j = 1, 2$. Then, the effective Hamiltonian in the continuum is given by

$$H = \int d^d \mathbf{x} \left(\frac{1}{2} [(\partial \phi_1)^2 + (\partial \phi_2)^2] \right). \quad (3)$$

The constraint $\phi_i \cdot \phi_j = \delta_{ij}$ for $i, j = 1, 2$ can be replaced by a soft potential $U(\phi_1, \phi_2)$ whose minima are given by $\phi_i \cdot \phi_j \propto \delta_{ij}$ and the Ginzburg-Landau-Wilson Hamiltonian for STA reads

$$H = \int d^d \mathbf{x} \left(\frac{1}{2} [(\partial \phi_1)^2 + (\partial \phi_2)^2] + U(\phi_1, \phi_2) \right). \quad (4)$$

Instead of ϕ_i , it is convenient to work with the invariants of the $O(N) \times O(2)$ group that can be chosen as:

$$\begin{aligned} \rho &= \text{Tr}({}^t \Phi \Phi) = \phi_1^2 + \phi_2^2, \\ \tau &= \frac{1}{2} \text{Tr}({}^t \Phi \Phi - \rho/2)^2 = \frac{1}{4} (\phi_1^2 - \phi_2^2)^2 + (\phi_1 \cdot \phi_2)^2. \end{aligned} \quad (5)$$

With this choice, the ground state configuration corresponds to $\rho = \text{const.}$ and $\tau = 0$. Up to the fourth order $U(\rho, \tau)$ can be written as

$$U(\rho, \tau) = \frac{\lambda}{2} (\rho - \kappa)^2 + \mu \tau, \quad (6)$$

where λ and μ are positive coupling constants. A typical ground state in terms of Φ is given by $\Phi_{\alpha, i} = \sqrt{\kappa/2} \delta_{\alpha, i}$, that is:

$$\Phi_{\min} \equiv \begin{pmatrix} \sqrt{\frac{\kappa}{2}} & 0 \\ 0 & \sqrt{\frac{\kappa}{2}} \\ \vdots & \vdots \\ 0 & 0 \end{pmatrix}. \quad (7)$$

III. THE NONPERTURBATIVE RENORMALIZATION GROUP EQUATION

The NPRG method is based on Wilson's idea of integrating statistical fluctuations step by step. In this paper, we employ the effective average action method as an implementation of the NPRG in continuum space [31–34].

The first step is to introduce a k -dependent partition function \mathcal{Z}_k in the presence of sources:

$$\mathcal{Z}_k[\mathbf{J}_i] = \int \mathcal{D}\phi_i \exp(-H[\phi_i] - \Delta H_k[\phi_i] + \mathbf{J}_i \cdot \phi_i), \quad (8)$$

where $\mathbf{J}_i \cdot \phi_i = \sum_{i=1}^2 \int_x \mathbf{J}_i(\mathbf{x}) \cdot \phi_i(\mathbf{x})$, and $\Delta H_k = 1/2 \sum_{i=1}^2 \phi_i(x) R_k(x-y) \phi_i(y)$. The idea underlying the effective average action is that in \mathcal{Z}_k only the fluctuations of large wave-numbers (the rapid modes) compared to k are integrated over while the others (the slow modes) are frozen by the ΔH_k term. As k is decreased, more and more modes are integrated until they are all when $k = 0$. The function $R_k(q^2)$, which is the Fourier transform of $R_k(x)$, plays the role of separating rapid and slow modes: It almost vanishes for $|q| > k$ so that the rapid modes are summed over and is large (of order k^2) below k so that the fluctuations of the slow modes are frozen. We define as usual $W_k[\mathbf{J}_i] = \ln \mathcal{Z}_k[\mathbf{J}_i]$. Thus, the order parameter $\varphi_j(\mathbf{x})$ at scale k is defined by

$$\varphi_i(\mathbf{x}) = \langle \phi_i(\mathbf{x}) \rangle = \frac{\delta W_k[\mathbf{J}_i]}{\delta \mathbf{J}_i(\mathbf{x})}. \quad (9)$$

The running effective average action $\Gamma_k[\varphi_i]$ is defined as the (modified) Legendre transform of W_k :

$$\Gamma_k[\varphi_i] = -W_k[\mathbf{J}_i] + \mathbf{J}_i \cdot \varphi_i - \Delta H_k[\varphi_i] \quad (10)$$

where \mathbf{J}_i is defined such that Eq. (9) holds for fixed φ_i . From this definition one can show that

$$\begin{cases} \Gamma_{k=\Lambda} \simeq H \\ \Gamma_{k=0} = \Gamma \end{cases}, \quad (11)$$

where the cutoff Λ is the inverse of the lattice spacing a . Equations (11) imply that Γ_k interpolates between the Hamiltonian of the system when no fluctuation has been summed over, that is, when $k = \Lambda$, and the Gibbs free energy Γ when they have all been integrated, that is, when $k = 0$. We define the variable t , called ‘‘RG time’’, by $t = \ln(k/\Lambda)$. The exact

flow equation for Γ_k reads [31, 32]:

$$\partial_t \Gamma_k[\varphi_i] = \frac{1}{2} \text{Tr} \int_{x,y} \partial_t R_k(x-y) \left(\frac{\delta^2 \Gamma_k[\varphi_i]}{\delta \varphi_i^\alpha(\mathbf{x}) \delta \varphi_{i'}^{\alpha'}(\mathbf{y})} + R_k(\mathbf{x}-\mathbf{y}) \delta_{i,i'} \delta_{\alpha,\alpha'} \right)^{-1}, \quad (12)$$

for $\alpha, \alpha' = 1, 2, \dots, N$ and $i, i' = 1, 2$.

IV. TRUNCATIONS OF THE NPRG EQUATION

It is generally not possible to solve exactly the above flow equation (12) and approximations are required in practice. In this paper, we employ the approximation of lowest level in the derivative expansion dubbed the local potential approximation (LPA) and some of its refinements.

Within the LPA, Γ_k is approximated by a series expansion in the gradient of the field, truncated at its lowest non trivial order:

$$\Gamma_k^{\text{LPA}}[\varphi_i] = \int d^d \mathbf{x} \left(\frac{1}{2} [(\partial \varphi_1)^2 + (\partial \varphi_2)^2] + U_k(\rho, \tau) \right). \quad (13)$$

Only a potential term $U_k(\rho, \tau)$ is thus retained in this approximation which is accurate as long as the impact of the renormalization of the derivative terms on the flow of the potential is small. This is most probably the case when the anomalous dimension is small and $d > 2$. The next level of approximation consists in including in the approximation a running field renormalization Z_k and a coupling constant ω_k , which affects the spectrum of a Goldstone mode around the minimum of the potential and is known to be important for the physics near $d = 2$ [1].

$$\Gamma_k = \int_x \left\{ U_k(\rho, \tau) + \frac{1}{2} Z_k \left((\partial \varphi_1)^2 + (\partial \varphi_2)^2 \right) + \frac{1}{4} \omega_k (\varphi_1 \cdot \partial \varphi_2 - \varphi_2 \cdot \partial \varphi_1)^2 \right\}. \quad (14)$$

This approximation has been used in [1, 21, 22, 35–37] where the function $U_k(\rho, \tau)$ was further expanded in powers of the invariants ρ and τ . This is what we improve here to avoid any artifact coming from this field truncation. This approximation, that we call LPA' with ω_k , yields the one-loop result obtained within the ϵ -expansion in $d = 4 - \epsilon$ and also the one-loop result of the $\epsilon = d - 2$ expansion of the nonlinear sigma model [1]. To examine the impact of including the coupling constant ω_k , we also make calculations setting $\omega_k = 0$ in Eq. (14): this approximation is called the LPA'.

The k -dependent effective potential $U_k(\rho, \tau)$ is defined by

$$\Omega U_k(\rho, \tau) = \Gamma_k[\varphi_i] \quad (15)$$

where $\varphi_i, i = 1, 2$ are constant fields and Ω is the volume of the system. The running field renormalization Z_k is set to one in LPA: $Z_k^{\text{LPA}} = 1$, which leads to a vanishing anomalous dimension: $\eta = 0$. In LPA' (or LPA' with ω_k) calculations, the anomalous dimension η is obtained from the flow of Z_k since it can be shown that at criticality:

$$Z_{k \rightarrow 0} \sim \left(\frac{k}{\Lambda}\right)^{-\eta}. \quad (16)$$

The flows of U_k, Z_k and ω_k have been derived in [1, 21, 22] and we give the expression in terms of $U_k(\rho, \tau)$ after some simplification in Appendix A. These flows are rather complicated and their numerical integration suffers from all the inherent difficulties of solving nonlinear partial differential equations.

The first difficulty comes from the choice of variables. It is tempting to work with the invariants ρ and τ defined above because the symmetry of the problem is encoded in the very definition of the variables and any smooth function of these variables corresponds to a function that has the right symmetry. However, ρ and τ satisfy $\frac{1}{4}\rho^2 \geq \tau \geq 0$ and it is not easy to deal with this constraint numerically because the domain where the variables ρ and τ live is nontrivial. Thus, we define another set of variables ψ_i which is numerically more convenient. For any φ_1 and φ_2 , it can be proven that there exists $O_1 \in O(N)$ and $O_2 \in O(2)$ such that the matrix $M \equiv O_1 \Psi O_2$, with the $N \times 2$ matrix Ψ defined as $\Psi = (\varphi_1, \varphi_2)$, becomes ‘‘diagonal’’, namely,

$$M \equiv \begin{pmatrix} \psi_1 & 0 \\ 0 & \psi_2 \\ \vdots & \vdots \\ 0 & 0 \end{pmatrix}. \quad (17)$$

Because of the $O(N) \times O(2)$ symmetry of the model, we conclude that $U_k(\Psi) = U_k(M)$. This fact shows that we can parametrize the order parameter space using ψ_1 and ψ_2 , instead of φ_1 and φ_2 . The $O(N) \times O(2)$ invariants ρ and τ are expressed in terms of ψ_1 and ψ_2 as

$$\begin{aligned} \rho &= \psi_1^2 + \psi_2^2 \\ \tau &= \frac{1}{4}(\psi_1^2 - \psi_2^2)^2. \end{aligned} \quad (18)$$

From the definitions (18), we find that the symmetries of the original problem imply:

$$U_k(\psi_1, \psi_2) = U_k(-\psi_1, \psi_2) = U_k(\psi_1, -\psi_2) = U_k(\psi_2, \psi_1). \quad (19)$$

Thus, to solve the flow equations, it is sufficient to consider the region $\psi_2 \geq \psi_1 \geq 0$. This triangular domain is much more convenient from a numerical point of view than the parabolic domain $\frac{1}{4}\rho^2 \geq \tau \geq 0$ for the invariants ρ and τ .

When the transition is of second order, the k -dependent effective action is attracted at criticality towards the fixed point solution of the NPRG flow equation once it is expressed in terms of the dimensionless renormalized fields $\tilde{\psi}_i$ and a dimensionless local potential $\tilde{U}_k(\tilde{\psi}_i)$. We thus define the dimensionless and renormalized quantities:

$$\begin{aligned} \tilde{\psi}_i &= (Z_k k^{2-d})^{1/2} \psi_i \\ \tilde{U}_k(\tilde{\psi}_i) &= k^{-d} U_k(\psi_i). \end{aligned} \quad (20)$$

The flow equation for \tilde{U}_k is given by Eq. (A3) in Appendix A. The critical exponent ν of the correlation length is obtained from the relevant eigenvalue of the linearized flow around the fixed point solution and η from the flow of Z_k . The other leading critical exponents can be deduced from these ones by scaling relations.

Throughout this paper we employ the following $R_k(\mathbf{q}^2)$:

$$R_k(\mathbf{q}^2) = \beta Z_k k^2 \left(1 - \frac{\mathbf{q}^2}{k^2}\right)^\alpha \Theta(k^2 - \mathbf{q}^2), \quad (21)$$

where we have introduced the parameters $\alpha \geq 1$ and $\beta > 0$, and Z_k is defined as

$$Z_k = \left(\frac{\partial}{\partial p^2} \left(\frac{\delta^2 \Gamma_k}{\delta \varphi_1^3(\mathbf{p}) \delta \varphi_1^3(-\mathbf{p})} / (2\pi)^d \delta(\mathbf{0}) \right) \right)_{\mathbf{p}=0, \min}, \quad (22)$$

where the field values are set to the minimum of U_k given by Eq. (7). The regulator function $R_k(\mathbf{q}^2)$ is useful for analytical treatments when $\alpha = \beta = 1$ [38] and is probably optimal at LPA [39]. We note that this family of regulators yields very accurate values of the critical exponents for $O(N)$ models at the fourth order of derivative expansion, after optimization based on PMS on α and β , as shown [40–42]), for example. Therefore we expect that Eq. (21) is also a good choice of regulator for $O(N) \times O(2)$ models. Here the Fourier transform $\phi_1^3(\mathbf{p})$ is defined as $\phi_1^3(\mathbf{p}) = \int d^d \mathbf{x} \phi_1^3(\mathbf{x}) \exp(-i\mathbf{x} \cdot \mathbf{q})$. The value of any physical quantity computed with a given regulator is independent of this regulator if the derivative expansion is not truncated to a finite order. However we do truncate it by

employing the LPA, LPA' and LPA' with ω_k , which are different approximations of the derivative expansion of the wavenumber dependent effective action Γ_k . Since the results at each level of the approximation are not exact, they depend on the choice of regulator, which explains why we perform the PMS optimization.

The dimensionless $O(N) \times O(2)$ invariants $\tilde{\rho}$ and $\tilde{\tau}$ are defined by $\tilde{\rho} = Z_k k^{2-d} \rho$, $\tilde{\tau} = Z_k^2 k^{2(2-d)} \tau$, and the potential and couplings by $\tilde{U}_k(\tilde{\rho}, \tilde{\tau}) = k^{-d} U_k(\rho, \tau)$, $\tilde{\omega}_k = Z_k^{-2} k^{d-2} \omega_k$, $y = q^2/k^2$, $R_k(q^2) = Z_k k^2 y r(y)$. Notice that as said above, Z_k does not reach a fixed point but η_k , defined by $\eta_k = -d \log Z_k / d \log k$, does: $\eta_{k \rightarrow 0} \rightarrow \eta$ at criticality with η the anomalous dimension of the fields. The flow of $\tilde{\omega}_k$ is also evaluated at the minimum of the potential.

V. NUMERICAL RESULTS

As said above, we use the variables $\tilde{\psi}_i$ defined in Eq. (20) to integrate the FP equations. These equations are discretized on a regular lattice and the domain corresponding to our numerical grid is a triangle in the $(\tilde{\psi}_1, \tilde{\psi}_2)$ plane of linear size $\tilde{\psi}_{\max}$ and mesh $\Delta\psi$. We have checked the convergence of all the numerical results presented below by varying these parameters.

A. The numerical method used to calculate the line $N_c(d)$

The line $N_c(d)$ separates in the (d, N) plane the region where the phase transition is of second order and the region where it is of first order. When the transition is of second order, a once-unstable FP called C_+ is associated with it. Two other nontrivial FPs are also found: the $O(2N)$ FP and a tricritical FP called C_- . The line $N_c(d)$ is the locus in the (d, N) plane where C_+ disappears by colliding with C_- : below this line, the RG flow was found to show a runaway which is the hallmark of a first-order transition [57].

There are two possibilities to determine $N_c(d)$. Either we decrease N at fixed d and look for the value of N where C_+ is no longer found and then repeat the same procedure by decreasing d . Or we compute the smallest eigenvalue of the flow around the fixed point C_+ corresponding to an irrelevant direction and look for the value of N where it vanishes. This eigenvalue is a measure of the speed of the flow on the RG trajectory joining C_+ and C_- and this speed goes to 0 when the fixed points collapse. We have used both methods and,

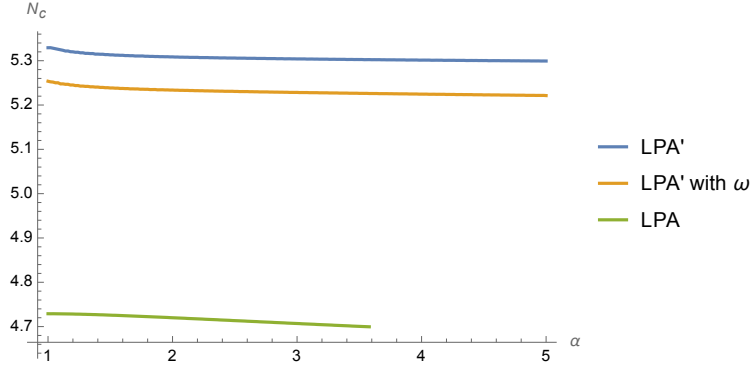


Figure 1: The curve $N_c(d = 3, \beta = 1, \alpha)$ at LPA, LPA' and LPA' with ω_k . Here we fix the parameter $\beta = 1$ and vary the parameter α in the regulator $R_k(q^2)$ defined in Eq. (21).

for the precision required in the present work, they are both satisfactory.

B. Calculation of $N_c(d = 3)$

We show $N_c(d = 3, \beta = 1, \alpha)$ at LPA, LPA' and LPA' with ω_k in Fig 1. This quantity does not have an extremum as a function of α . When such a quantity has an extremum as a function of a tunable and unphysical parameter such as α , this extremum is interpreted as the optimal value of this quantity because it corresponds to the region of smallest dependence upon the parameter (Principle of Minimal Sensitivity). When applied to $O(N)$ models, this principle allows accurate determination of the critical exponents [40–42]. As can be seen on Fig. 1, there is no extremum but the magnitude ΔN_c of the variation of N_c is very small, smaller than 0.1, when α is varied on a large range of values, typically between 1 and 5. Consequently, the uncertainty associated with the choice of regulator seems much smaller than that associated with the truncation of the DE at either LPA or LPA' or LPA' with ω_k , considering the variations of this quantity from one approximation scheme to another. We therefore retain the values: $N_c(d = 3) \simeq 4.7, 5.3$ and 5.2 for respectively the LPA, LPA' and LPA' with ω_k . We note that Zumbach in [19] already obtained $N_c(d = 3) \simeq 4.7$ at LPA implemented on the Polchinski equation without any field expansion. These values of $N_c(d = 3)$ are almost compatible with $N_c^{\text{semi}}(d = 3) \simeq 4.68(2), 5.24(2)$ obtained from a “semi-expansion” [22] within LPA and LPA' with ω_k , respectively. In the semi-expansion approximation, the potential is treated functionally in the ρ -direction but expanded in the τ -direction. This expansion is found to converge nicely at small orders in τ for $d \geq 3$. In

[22], another regulator called the exponential regulator was employed, instead of Eq. (21) used in the present study:

$$R_k^{\text{exp}}(\mathbf{q}^2) = Z_k \alpha' \mathbf{q}^2 / (e^{\mathbf{q}^2/k^2} - 1). \quad (23)$$

For this regulator, the semi-expansion is expected to almost converge in $d = 3$ within LPA and LPA' with ω_k . Therefore, the fact that the two studies give almost the same values of $N_c(d)$ suggests that the dependence of $N_c(d)$ on the choice of the regulator is very small and $N_c(d)$ is rather precisely determined within each approximation (LPA, LPA' or LPA' with ω_k), at least for $d \geq 3$. The remaining source of error is the field dependence of the second order derivative terms, which is not fully taken into account in the current approximations, and the higher order derivative terms in Γ_k . Therefore, the discrepancy on $N_c(d)$ between NPRG and the ϵ -expansion might be improved with full calculation at second order of derivative expansion on the side of NPRG, as a first step.

C. Critical exponents ν and η for $N = 6$ and $d = 3$

We show the critical exponent $\nu(d = 3, N = 6, \beta = 1, \alpha)$ at LPA, LPA' and LPA' with ω_k in Fig 2. As α increases in the interval $1 < \alpha < 5$, ν increases and does not have an extremum. To see whether the absence of an optimal value is due to the particular choice of the parameters, we have calculated $\nu(d = 3, N = 6, \beta, \alpha = 2)$ for several values of the prefactor β while fixing the exponent $\alpha = 2$ (data not shown) and we did not find an optimal value either. On the other hand, in semi-expansion [22], $\nu(d = 3, N = 6)$ varies typically between 0.69 and 0.73 at LPA' with ω_k depending on the parameter in the exponential regulator. As a function of α' in Eq. (23), the authors have found that there is no optimal value of the exponent but for large values of α' the variation of $\nu(d = 3, N = 6, \alpha')$ is rather small. From this observation, they concluded that an estimate of the exponents is $\nu^{\text{semi}}(d = 3, N = 6) = 0.695(5)$ and $\eta^{\text{semi}} = 0.042(2)$. Using the regulator in Eq. (21) with $\beta = 1$, we find at LPA' with ω_k a PMS value for η at $\alpha \simeq 2$: $\eta(\alpha = 2) = 0.0457$, see Fig. 3. For this value of α , we find $\nu(\alpha \simeq 2) \simeq 0.727$, see Fig. 2. Provided that the previous results obtained with the semi-expansion were converged, the difference between the two sets of results given above must come from the choice of regulators. We conclude that contrary to the value of $N_c(d = 3)$, the variations of the critical exponents with the regulator is not

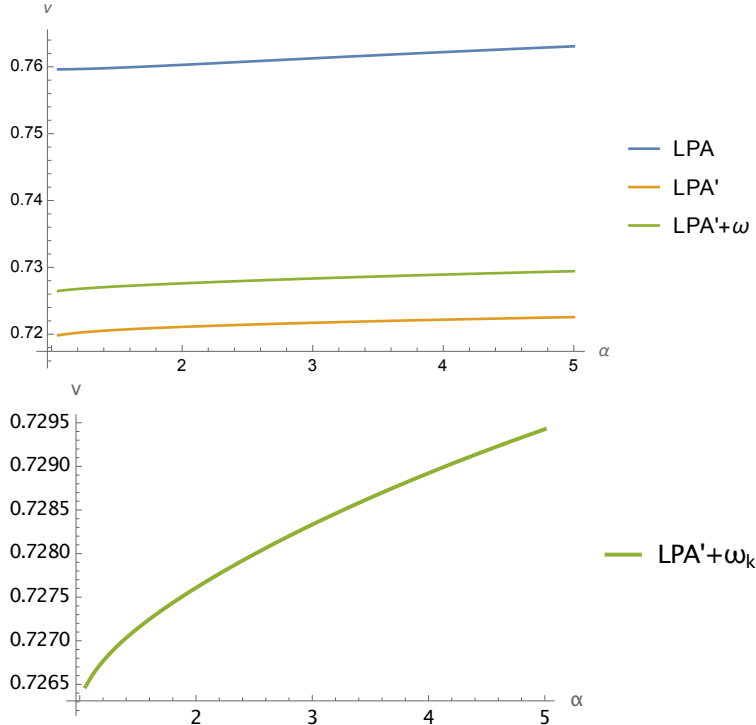


Figure 2: The critical exponent $\nu(d = 3, N = 6, \beta = 1, \alpha)$ at LPA, LPA' and LPA' with ω_k . Here we fix the parameter $\beta = 1$ and vary the parameter α in the regulator $R_k(q^2)$. We do not have PMS.

very small, at least for $N = 6$. On the other hand, the values of ν and η given above are compatible with the bounds given by the conformal bootstrap [26]. We have checked that for $N = 7$ and $N = 8$, our results for both ν and η differ at most by 10% from the 6-loop ϵ -expansion results and from the Monte Carlo simulations [43, 44]. Notice that such an error of about 10% in $d = 3$ is expected at the level of the LPA' since this is typically what is found in $O(N)$ models and in models whose upper critical dimension is four [39].

D. Calculation of $N_c(d = 2.5)$

As mentioned in the Introduction, it is interesting to study the shape of the curve $N_c(d)$ below $d = 3$ to find out whether or not it shows a S-shape and thus a possible re-entrance of the first order region below the value of $N_c(d = 3)$ found above. On the example of the dimension $d = 2.5$, we show in this section that our solution of the LPA' with ω_k FP equations is numerically well under control.

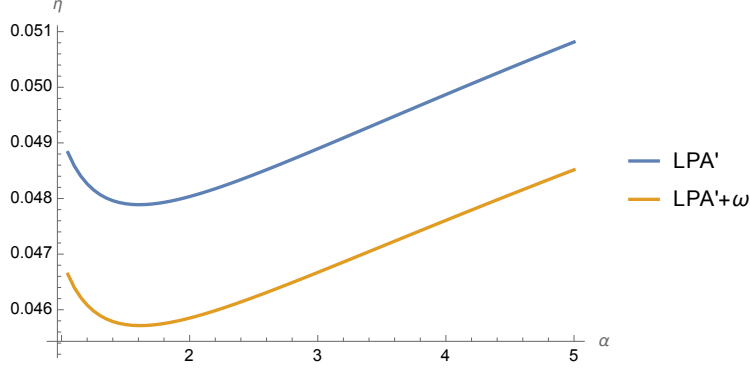


Figure 3: The critical exponent $\eta(d = 3, N = 6, \beta = 1, \alpha)$ at LPA' and LPA' with ω_k . Here we fix the parameter $\beta = 1$ and vary the parameter α in the regulator $R_k(q^2)$. We have PMS around $\alpha = 1.6$.

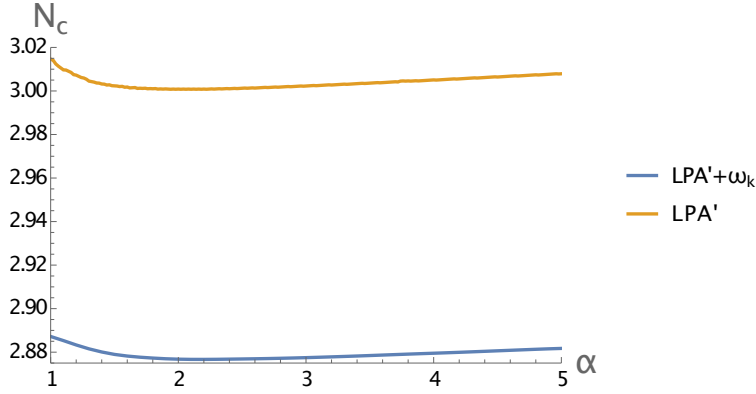


Figure 4: The curve $N_c(d = 2.5, \beta = 1, \alpha)$ at LPA' and LPA' with ω_k . Here we fix the parameter $\beta = 1$ and vary the parameter α in the regulator $R_k(q^2)$.

As previously emphasized, the LPA is not sufficient to recover the one-loop result in $d = 2 + \epsilon$ and the LPA' with ω_k is mandatory. In the following, we focus on this approximation as well as on the LPA' when we study $N_c(d)$ in low dimensions.

We show $N_c(d = 2.5, \beta = 1, \alpha)$ at LPA' with ω_k in Fig 4. At LPA' and LPA' with ω_k , a minimum as a function of α exists respectively at $N_c^{\text{opt}}(d = 2.5, \beta = 1, \alpha \simeq 2) = 3.00$ and $N_c^{\text{opt}}(d = 2.5, \beta = 1, \alpha \simeq 2) = 2.88$.

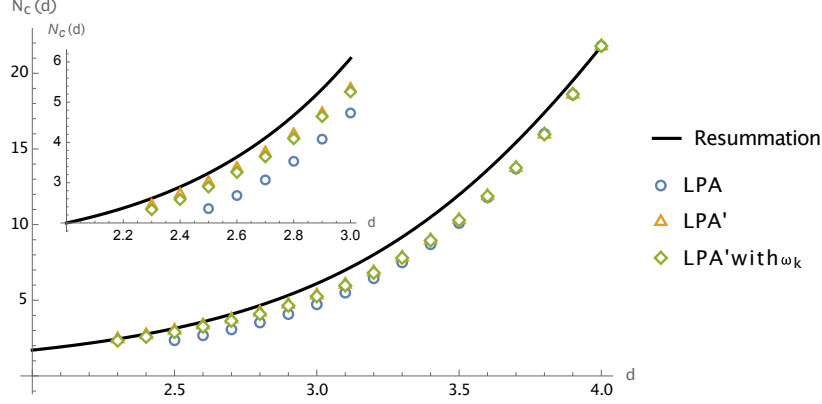


Figure 5: The curve $N_c(d, \alpha = 1, \beta = 1)$. The continuous curve corresponds to the resummed five-loop ϵ -expansion [18]. The spreading of values of $N_c(d, \alpha, \beta)$ when α is varied between 1 and 5 and β between 1 and 2 is almost invisible on this scale.

E. The curve $N_c(d)$ in $2.3 \leq d \leq 4$

We have found that it becomes more and more difficult to obtain converged results when decreasing the dimension. We have been able to decrease d down to 2.3 but not below with the LPA' with ω_k . As discussed in Appendix B 4, the numerical difficulty is due to the steep increase of the FP potential at large fields. It would be interesting to improve our numerical scheme explained in detail in Appendix B, in the future, in order to approach $d = 2$ further. We show our determination of $N_c(d)$ in Fig. 5 together with the results obtained from the ϵ -expansion at five loops [58].

For $d = 3$, our results confirm the previous results obtained either by NPRG [1, 19–22] or the ϵ -expansion approaches [18, 45, 46]. The comparison between the LPA and LPA' results strongly suggests that neglecting the effect of the derivative terms on the determination of $N_c(d)$ plays a minor role in $d = 3$ as for the order of the transition for $N = 2$ and $N = 3$. Moreover, $N_c(d = 3)$ increases between the LPA and the LPA' with ω_k and becomes closer to the results obtained with the ϵ -expansion, which is expected. It seems therefore very difficult to imagine that $N_c(d = 3)$ could be smaller than 3. Judging from the curve $N_c(d)$ for $2.3 \leq d \leq 4$, it also seems very unlikely that $N_c(d)$ has a turn around point and is a multi-valued function around $d = 3$, which is one of the expected scenarios to allow for the existence of C_+ in $d = 3$ and $N = 3$.

F. Comments on estimation of the error bars

Although, throughout this paper, we qualitatively estimate the error of our calculation using the dispersion of the results when the regulator and the approximation (LPA, LPA' or LPA' with ω_k) are varied, the quantitatively reliable error bars can only be computed by comparing two successive orders of the derivative expansion. Our calculations, limited to LPA and LPA', are not sufficient to quantitatively estimate the error bars of $N_c(d)$. However, the same thing happens for critical exponents with LPA', which nevertheless gives fairly accurate results that are, say, within 10% of the exact values (as given by the conformal bootstrap).

VI. CONCLUSION

Let us also emphasize that the only Monte Carlo simulations that still find a second order transition for a value of N below our value of $N_c(d=3)$, that is, for $N \leq 4$, has been performed for $N = 2$ by Calabrese et al. [17] on a discretization of the Ginzburg-Landau model Eqs. (4), (6) and by Nagano and Kawamura [8] on Heisenberg STA. Calabrese et al found that depending on the values of the parameters λ and μ in Eq. (6), the transition is of first or second order: At fixed λ and small μ , the transition is of second order whereas it is of first order at large μ . Since nonuniversal quantities, such as phase diagrams [47, 48], can be accurately computed from the integration of the NPRG flow equations, it is possible to estimate the magnitude of the correlation length ξ at the transition within the LPA' by initializing the flow with the data corresponding to the simulations. By varying these data as well as the cut-off function $R_k(q)$, it is found that ξ is always finite (since there is no fixed point) but very large, typically larger than 2000 lattice spacings [49]. From a numerical point of view, there is no doubt that such a large correlation length makes it impossible to decide in favor of a second or a very weak first order phase transition since in both cases the physics looks the same at the scale of the lattice size which was at most 384 lattice spacings in the numerical simulations. We conclude that this Monte Carlo result does not contradict our conclusion that $N_c(d=3) \gtrsim 5$.

This result shows unambiguously that if our result is wrong, the origin of the problem can only be found by including the renormalization of the functions in front of the derivative

terms. However, considering that the anomalous dimension is small for these systems when they undergo a second order phase transition, that is, for $N > N_c$, this hypothesis seems very doubtful. We suggest that the Blaizot-Mendez-Wschebor approach [50–52], where the full momentum dependence of the two-point functions is retained as well as the full field-dependence of the potential \tilde{U} could lead to a very accurate determination of $N_c(3)$.

As for the approach to $d = 2$, we find a remarkable agreement between our results and what was found within the ϵ -expansion where two resummations were performed in [18], either by assuming that $N_c(d = 2) = 2$ or by letting free the value of $N_c(d = 2)$, see Fig. 5. This agreement is not very surprising because we expect the LPA' with ω_k to be one-loop exact in $d = 2 + \epsilon$ for $N > 2$. Notice that our results are not precise enough to determine unambiguously the value of $N_c(d = 2)$ although it seems clear that it cannot be very different from 2. It is therefore very unlikely that $N_c(d = 2) > 3$. Since the NPRG flow reproduces the low-temperature expansion of the nonlinear sigma model around $d = 2$, we conclude that the critical behavior of frustrated systems in $d = 2 + \epsilon$ is driven for $N = 3$ by the fixed point C_+ corresponding to a critical temperature of order ϵ in agreement with Mermin-Wagner theorem. Since we find no other once-unstable fixed point, we conclude that our study rules out the possibility of having a finite temperature fixed point in $d = 2$ for $N = 3$ contrary to what was found at five loops in a fixed dimension RG calculation [9].

To conclude, we have presented a rather simple method to compute the FP properties of matrix models describing frustrated systems without having recourse to a field expansion of the free energy Γ (but keeping a derivative expansion of Γ). This is especially important in low dimensions where the field expansion is known to fail. In dimension $d = 3$, our results fully confirm what was previously found within less accurate NPRG calculations that involved field truncations on top of the derivative expansion [1, 21, 22]. In dimension $d = 2$, more stable numerical schemes are still needed to study the physics of topological excitations in frustrated systems (that are of different natures than in nonfrustrated systems) and we believe that the present work is the first step in this direction. With field expansion, we studied the fate of the C_- FP in dimensions lower than 3 and found that it vanishes by colliding with another multicritical FP [53]. Since multicritical FPs show in their FP potential boundary layer at Large- N in $O(N)$ models [54, 55], which needs functional treatment, it would be also important to study functionally the multicritical FPs in the frustrated cases. Finally, let us mention that there are many systems with multiple invariants whose two-

dimensional physics can only be studied functionally in the NPRG framework [56]. Similar procedures to that presented in this work might be useful for such models.

VII. ACKNOWLEDGMENT

This work was supported in part by a Grant-in-Aid for Young Scientists (B) (15K17737), Grants-in-Aid for Japan Society for Promotion of Science (JSPS) Fellows (Grants Nos. 241799 and 263111), the JSPS Core-to-Core Program "Non-equilibrium dynamics of soft matter and information".

Appendix A: The nonperturbative renormalization group flow equations and the anomalous dimension

Since the explicit expression of flow equations is rather complicated except when the Litim regulator ($\alpha = \beta = 1$) is taken and $\omega_k = 0$, we present them only for $\alpha = \beta = 1$ and $\omega_k = 0$. See [22] for the complete expressions at LPA' with $\omega_k \neq 0$. Then, the running anomalous dimension $\eta_k = -k\partial_k Z_k$ is given, at the level of LPA', by

$$\eta_k = 64 \frac{\tilde{\kappa} v_d}{d} \left(2 \left(\frac{\tilde{U}_k^{(2,0)'}}{1 + 4\tilde{\kappa}\tilde{U}_k^{(2,0)'}} \right)^2 + \left(\frac{\tilde{U}_k^{(0,1)'}}{1 + 2\tilde{\kappa}\tilde{U}_k^{(0,1)'}} \right)^2 \right), \quad (\text{A1})$$

where we set $\tilde{\rho} = \tilde{\kappa}$ and $\tilde{\tau} = 0$. The derivatives $\tilde{U}_k^{(i,j)'}$ with respect to the invariants $\tilde{\rho}$ and $\tilde{\tau}$, and v_d are defined as

$$\tilde{U}_k^{(i,j)' } \equiv \frac{\partial^{i+j}\tilde{U}_k}{\partial\tilde{\rho}^i\partial\tilde{\tau}^j}, \quad v_d = \frac{1}{2^{d+1}\pi^{d/2}\Gamma\left(\frac{d}{2}\right)}.$$

The nonperturbative renormalization group flow equation for the potential \tilde{U}_k is given

by

$$\begin{aligned}
\partial_t \tilde{U}_k &= -d\tilde{U}_k + \frac{1}{2}(-2 + d + \eta_k) \left(\tilde{\psi}_1 \tilde{U}_k^{(1,0)} + \tilde{\psi}_2 \tilde{U}_k^{(0,1)} \right) \\
&\quad + \frac{4(2 + d - \eta_k)}{d(2 + d)} v_d \\
&\quad \times \left(\frac{\tilde{\psi}_1 - \tilde{\psi}_2}{\tilde{\psi}_1 - \tilde{\psi}_2 - \tilde{U}_k^{(0,1)} + \tilde{U}_k^{(1,0)}} + \frac{\tilde{\psi}_1 + \tilde{\psi}_2}{\tilde{\psi}_1 + \tilde{\psi}_2 + \tilde{U}_k^{(0,1)} + \tilde{U}_k^{(1,0)}} \right) \\
&\quad + (N - 2) \left(\frac{\tilde{\psi}_2}{\tilde{\psi}_2 + \tilde{U}_k^{(0,1)}} + \frac{\tilde{\psi}_1}{\tilde{\psi}_1 + \tilde{U}_k^{(1,0)}} \right) \\
&\quad + \frac{2 + \tilde{U}_k^{(0,2)} + \tilde{U}_k^{(2,0)}}{1 - \left(\tilde{U}_k^{(1,1)} \right)^2 + \tilde{U}_k^{(2,0)} + \tilde{U}_k^{(0,2)} \left(1 + \tilde{U}_k^{(2,0)} \right)} \Bigg). \tag{A2}
\end{aligned}$$

Here, to simplify the notation, we have defined another kind of derivatives $\tilde{U}_k^{(i,j)}$ with respect to $\tilde{\psi}_1$ and $\tilde{\psi}_2$ as

$$\tilde{U}_k^{(i,j)} \equiv \frac{\partial^{i+j} \tilde{U}_k}{\partial \tilde{\psi}_1^i \partial \tilde{\psi}_2^j}. \tag{A3}$$

In our calculations, we use the rescaled potential $v_d^{-1} \tilde{U}_k$ and fields $(v_d)^{-1/2} \tilde{\psi}_i$ for $i = 1, 2$ in such a way that v_d disappears in Eqs (A1) and (A2).

Appendix B: Numerical methods

1. The fixed point at LPA

To simplify the explanation, we focus on LPA in this subsection. From a numerical point of view, there are two possibilities for finding fixed points when they exist.

The first is to dynamically integrate the flow. In this case, the problem is to find the critical surface which is usually done by dichotomy on the temperature. Once it is found, the fixed point is (approximately) reached since it is attractive on the critical surface. The approximation of the FP found this way can be used as an initial condition for a direct search of the FP by a Newton-Raphson method if it is necessary to refine the numerical accuracy.

The other method is to look directly for the solution of the fixed point equation (coupled with Eq. (A1)): $\partial_t \tilde{U}^*(\tilde{\psi}_i) = 0$. This is what we do here. The advantage of this method is three-fold: (i) The numerical scheme is much simpler than integrating the flow; (ii) several

numerical instabilities occurring during the integration of the flow are avoided; (iii) the critical exponents are easily obtained from the diagonalization of the RG flow around the fixed point. We show in the following that although this scheme works very well in dimension $d = 3$, numerical difficulties arise in dimensions close to $d = 2$, making it almost impossible to study the physics of frustrated systems in this dimension, at least with our numerical scheme.

The basic idea of this scheme is simple. It consists in solving the FP equations for \tilde{U}^* on a grid in (ψ_1, ψ_2) space, taking into account the symmetries (19). We introduce a cut-off field value $\tilde{\psi}_{max}$ and consider the triangular domain $D : \tilde{\psi}_{max} \geq \tilde{\psi}_2 \geq \tilde{\psi}_1 \geq 0$. We then discretize D on a square lattice with mesh size $\Delta\tilde{\psi} = \tilde{\psi}_{max}/(N_p - 1)$, where N_p is the number of lattice points on the axis $\psi_1 = 0$. The lattice points are given by $(i\Delta\tilde{\psi}, j\Delta\tilde{\psi})$ for integers i and j that satisfy $0 \leq i \leq j \leq N_p - 1$. We define $\tilde{U}_t(i, j) \equiv \tilde{U}_t(i\Delta\psi, j\Delta\psi)$ to alleviate the notation.

The fixed point equation for the potential is a differential equation. We transform it into a set of algebraic equations by discretizing the derivatives of \tilde{U} . We give below some details about this procedure because all our numerical problems come from the boundary of the domain D , precisely at the points where the discretization involves exceptional cases.

The formulae for the derivatives $\tilde{U}_t^{(l,m)}(i, j)$ for $l, m = 0, 1, 2$ are constructed as follows:

(1) In the bulk region ($0 \leq i \leq j \leq N_p - 3$): $U^{(1,0)}$ and $U^{(2,0)}$ as well as $U^{(0,1)}$ and $U^{(0,2)}$ are computed with five points. $U^{(1,1)}$ is computed with the nine points $\tilde{U}_t(i, j)$, $\tilde{U}_t((i \pm 1), (j \pm 1))$, $\tilde{U}_t((i \pm 1), (j \mp 1))$, $\tilde{U}_t((i \pm 2), (j \pm 2))$ and $\tilde{U}_t((i \pm 2), (j \mp 2))$. The formulae are exact up to $(\Delta\psi)^3$. Notice that for points on the two borders of D defined either by $\tilde{\psi}_1 = 0$ or $\tilde{\psi}_1 = \tilde{\psi}_2$, the derivatives of \tilde{U} involve points outside D . By using (19), we can compute these values of \tilde{U} from those that are inside D . This is one of the advantage of the choice of variables (ψ_1, ψ_2) compared to the choice (ρ, τ) : The derivatives on the two borders $\tilde{\psi}_1 = 0$ and $\tilde{\psi}_1 = \tilde{\psi}_2$ can be computed in the same way as in the bulk.

(2) On the boundary of the domain D corresponding to the large field region, $j = N_p - 2, N_p - 1$, we compute the derivatives in the ψ_1 direction $U^{(1,0)}(i, j)$ and $U^{(2,0)}(i, j)$ in the same way as in (1), that is, as in the bulk. The formulae for $U^{(0,1)}(i, j)$ and $U^{(0,2)}(i, j)$ are constructed with the five quantities $\tilde{U}_t(i, j')$ for $j' = N_p - 5, \dots, N_p - 1$ and are exact at order $(\Delta\psi)^2$. The formula for $U^{(1,1)}(i, N_p - 1)$ for $0 \leq i \leq N_p - 2$ involves the six values $\tilde{U}_t(i + 1, j')$, $\tilde{U}_t(i - 1, j')$ for $j' = N_p - 3, N_p - 2, N_p - 1$ and is exact at order $(\Delta\psi)$. Finally, for $U^{(1,1)}(N_p - 1, N_p - 1)$ we use twelve points in the region $N_p - 4 \leq i \leq j \leq N_p - 1$ and

the formula is exact at order $(\Delta\psi)^2$.

Notice that we have increased the precision of the derivatives on the boundary of the domain D corresponding to the large field region in order to test the robustness of our results with respect to the choice of discretization and to try to reduce numerical problems when d is close to 2. In all cases studied we did not find any significant changes. In particular, the scheme is not more stable when the number of points chosen to compute the derivatives is increased.

Once the derivatives are discretized, the fixed point equation $\partial_t \tilde{U}^*(\psi_1, \psi_2) = 0$ becomes a set of coupled algebraic equations for $g_{i,j}^* \equiv \tilde{U}^*(i, j)$. We look for a solution to these equations by a Newton-like method. One of the difficulty of this method is the huge number of unknowns and the possibility for Newton's method to get lost in the very complicated landscape of extrema of the set of equations to be solved. The way out of this difficulty is to deform continuously a solution of the problem.

Our strategy in this paper is to follow the fixed point potential $\tilde{U}^*(\tilde{\psi}_1, \tilde{\psi}_2)$ by changing the dimension d and the number of spin components N gradually starting from $d = 3.9$ and $N = 22$ where the field-expansion method provides a good approximation of the fixed point potential. We use as an initial condition of Newton's method:

$$\tilde{U}^{*,\text{init}}(\tilde{\psi}_1, \tilde{\psi}_2) = \frac{\tilde{\lambda}^*}{2} (\tilde{\rho} - \tilde{\kappa}^*)^2 + \tilde{\mu}^* \tilde{\tau} \quad (\text{B1})$$

and $\eta = 0$. The parameters $\tilde{\lambda}^*$, $\tilde{\kappa}^*$ and $\tilde{\mu}^*$ are determined by performing a field-expansion of the LPA equation on \tilde{U} at order four in the fields and solving the fixed point equation for these parameters in $d = 3.9$ and for $N = 22$. As expected, we find four fixed points: the Gaussian and the $O(2N)$ fixed points as well as a once-unstable fixed point C_+ driving the phase transition and C_- that corresponds to a tricritical fixed point. Once an approximation of C_+ is found with the truncation of Eq. (B1), we use it as the initial condition of Newton's method for the full potential equation and we easily find \tilde{U}^* . Then, we move in the (d, N) plane by little steps using as new initial condition what was found for the previous value of d and/or N studied. The fixed potential potential deforms smoothly and the Newton's method always works properly this way. We give a plot of the FP potential for the C_+ FP for $d = 3$ and $N = 8$ at LPA in Fig. 6.

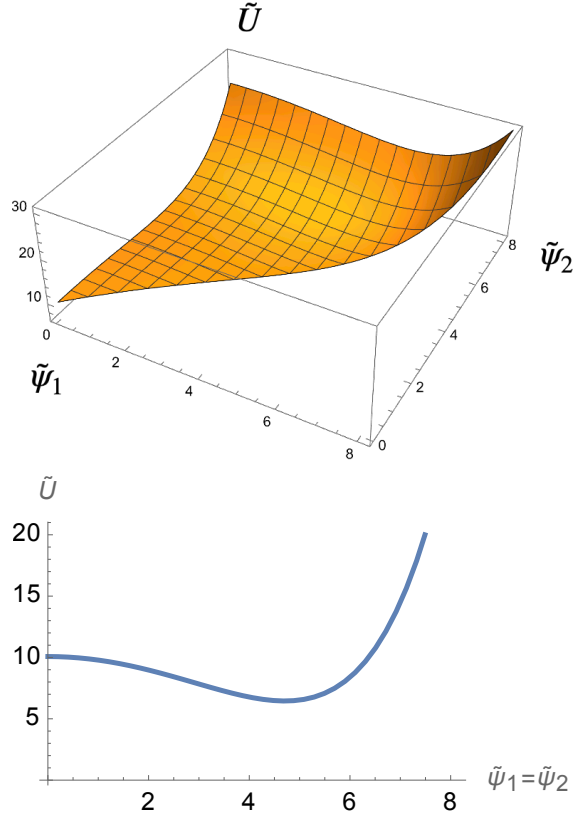


Figure 6: (Top) The FP potential $\tilde{U}^*(\tilde{\psi}_1, \tilde{\psi}_2)$ of the C_+ FP for $d = 3$ and $N = 8$ at LPA. (Bottom) The FP potential $\tilde{U}^*(\tilde{\psi}_1, \tilde{\psi}_1)$ on the diagonal line $\tilde{\psi}_1 = \tilde{\psi}_2$ of the same FP. The minimum of the potential locates at $(\tilde{\psi}_1, \tilde{\psi}_2) = (4.68, 4.68)$.

2. Eigenvalues of the stability matrix around a fixed point

For each value of (d, N) studied, we compute the eigenvalues of the stability matrix $\Theta(\{i, j\}, \{i', j'\})$ defined as

$$\Theta(\{i, j\}, \{i', j'\}) \equiv \frac{\partial (\partial_t g_{\{i, j\}}(t))}{\partial g_{\{i', j'\}}(t)} \Big|_{g_{i, j}^*} \quad (\text{B2})$$

where we consider $\{i, j\}$ and $\{i', j'\}$ as (super-)indices. Since the RG time $t = \log k/\Lambda$ is negative, a negative (positive) eigenvalue of the matrix Θ corresponds to a relevant (irrelevant) eigendirection around the fixed point. We sort the eigenvalues as $\sigma_0 (= -d) < \sigma_1 < \dots < \sigma_{i-1} < \sigma_i < \dots$. Note that the above stability matrix around any fixed point solution has a trivial relevant eigendirection corresponding to the constant shift $g_{i, j} = g_{i, j}^* + \text{const}$ with the eigenvalue $\sigma_0 = -d$, which can be easily seen from Eq. (A3). Hereafter, this trivial eigenvalue is omitted when we discuss the stability of a fixed point. The critical exponent ν

is given by $\nu = -1/\sigma_1$ and the smallest positive eigenvalue that vanishes when C_+ collapses with C_- is σ_2 .

3. Extension to LPA' and LPA' with ω_k

In this subsection we briefly explain how we extend, for LPA' and LPA' with ω_k , the procedure to calculate the FP solution and the eigenvalues of the stability matrix at LPA. At LPA' and LPA' with ω_k , we have to take into account $\eta \neq 0$ and the flow of ω_k , which are evaluated at the minimum of the potential $(\rho, \tau) = (\kappa, 0)$. Note that κ is determined as a function of $g_{i,j}$. Therefore the coupling constants that we have to consider here are $g_{i,j}$ and ω_k . The flow of $g_{i,j}$ or ω_k can be obtained as a function of $g_{i,j}$ or ω_k with the same discretization procedure described so far. At a given (d, N) , by recursively adjusting $\tilde{\psi}_{max}$, the minimum of the potential locates exactly on a lattice point, so that all the derivatives $U_{i,j}^{(k,l)}$ at the minimum can be evaluated with the procedure explained in the subsection B 1. With this $\tilde{\psi}_{max}$, we find the FP solution. To evaluate the stability matrix for these flow equations, we calculate $\frac{\partial \kappa(t)}{\partial (\partial_t g_{\{i,j\}}(t))} |_{g_{i,j}^*, \omega_k}$ as follows: The perturbation around the FP $g_{i,j} \rightarrow g_{i,j}^* + \delta g_{i,j}$ changes the location of the minimum as $\kappa \rightarrow \kappa + \delta \kappa$. Since $\partial(U_k^* + \delta U_k)(\rho = \kappa + \delta \kappa, 0)/\partial \rho = 0$, at the linear order of perturbation, we have

$$\delta \kappa = - \frac{\partial \delta U(\rho = \kappa, 0)}{\partial \rho} / \frac{\partial^2 U^*(\rho = \kappa, 0)}{\partial \rho^2}, \quad (\text{B3})$$

which can be evaluated in terms of $g_{i,j}^*$ and $\delta g_{i,j}$ using the expressions of the discretized derivatives of U presented in the previous subsection B 1. This leads to the desired discretized expression of $\frac{\partial \kappa(t)}{\partial (\partial_t g_{\{i,j\}}(t))} |_{g_{i,j}^*, \omega_k}$.

4. Numerical instabilities

For each dimension d and value of N we have to make sure that our results are converged. First we focus on LPA with Litim cutoff. Once the choice of discretization of the derivatives has been made, there are two parameters that can be tuned: the values of $\tilde{\psi}_{max}$ and of the mesh size $\Delta \tilde{\psi} = \tilde{\psi}_{max}/(N_p - 1)$. The potential \tilde{U}^* shows a minimum at $\tilde{\psi}_1 = \tilde{\psi}_2 = \tilde{\psi}_{min}$ and we have observed that $\tilde{\psi}_{max}$ should be at least 1.5 times larger than $\tilde{\psi}_{min}$ to get values of $N_c(d)$ converged with an accuracy of at least 1%. We have also observed that the smaller

$N_p = 61$	$-3, -1.45, 0.218, 0.827, 1.99, 2.79$	(B4)
	$-0.464 \pm 34.8i, 0.250 \pm 30.9i, 1.07 \pm 27.6i$	
$N_p = 81$	$-3, -1.45, 0.218, 0.827, 1.99, 2.79$	
	$0.059 \pm 47.9i, 0.868 \pm 43.5i, 1.76 \pm 39.9i$	
$N_p = 101$	$-3, -1.45, 0.218, 0.827, 1.99, 2.79,$	
	$0.704 \pm 61.05i, 1.627 \pm 56.3i$	

Table I: Several of the most relevant eigenvalues around the C_+ fixed point for $N = 5$ and $d = 3$ at LPA with Litim cutoff. We have chosen $\tilde{\psi}_{max} = 9/4\tilde{\psi}_{min}$. The physical eigenvalues are given on the first line for each value of N_p and the others, that are spurious, on the second line. For $N_p = 61$, the eigenvalues $-0.464 \pm 34.8i$ are relevant since their real part is negative. This eigenvalue disappears when increasing N_p , as it should.

the dimension, the smaller $\Delta\tilde{\psi}$ must be to get converged results. This last point has two origins. First, for d close to 2, the FP potential is steep at large fields because it behaves as $(\tilde{\psi}_1^2 + \tilde{\psi}_2^2)^{\frac{d}{d-2+\eta}}$ and a small mesh size is necessary to accurately describe the shape of \tilde{U}^* . Second, if N_p is too small, we find that even far away from $d = 2$, say $d = 3$, several eigenvalues corresponding to relevant eigendirections appear in the spectrum and spoil the degree of stability of the fixed point C_+ . These eigenvalues are clearly spurious because their values change considerably when either $\Delta\tilde{\psi}$ is decreased or $\tilde{\psi}_{max}$ is increased whereas the complementary set of eigenvalues, the physical ones, remain unchanged up to the sixth digit, see Table I. We observe that as $\Delta\tilde{\psi}$ is decreased, these spurious eigenvalues systematically disappear (or, at least, get a very large real part which makes them highly irrelevant). The conclusion of this study is that for each d , a sufficiently large N_p should be chosen so that the set of first most relevant eigenvalues is converged as for their numbers and values. In particular, when the numerical results are converged all spurious relevant eigenvalues have disappeared. We find that in $d = 3$, $N_p = 101$ is sufficient to get fully converged results while leading to numerically feasible calculations, when we take $\tilde{\psi}_{max} = 2.27\tilde{\psi}_{min}$. We also find that as d approaches 2, “large” values of $\tilde{\psi}_{max}$ favor the presence of spurious eigenvalues that can only be eliminated by increasing N_p . It turns out that around $d = 2.4$, very large values of N_p , such as $N_p = 200$, would be necessary to avoid spurious eigenvalues and that

decreasing d would impose to increase N_p in a prohibitive way. This is why we did not determine $N_c(d)$ at LPA for $d < 2.5$.

Next we discuss LPA' and LPA' with ω_k . Note that the problem of spurious eigenvalues encountered at LPA becomes less severe for LPA' and LPA' with ω_k , since $\eta \neq 0$ which implies that the FP potential is less steep at large fields than at LPA. Typically, when we take $\tilde{\psi}_{max} \simeq 1.5\tilde{\psi}_{min}$, $N_p = 40$ in $d = 2.4$ is sufficient to avoid spurious eigenvalues with negative real part. We have been able to compute $N_c(d)$ down to $d = 2.3$ by computing directly the value of N where no fixed point C_+ is found with Newton's method but we have not been able to go below this dimension.

-
- [1] B. Delamotte, D. Mouhanna, and M. Tissier, Phys.Rev. B **69**, 134413 (2004).
 - [2] H. Kawamura, Journal of Physics: Condensed Matter **10**, 4707 (1998).
 - [3] M. Yosefin and E. Domany, Phys. Rev. B **32**, 1778 (1985).
 - [4] D. Loison and K. D. Schotte. Eur. Phys. J. B **5**, 735 (1998).
 - [5] D. Loison and K. D. Schotte. Eur. Phys. J. B, **14**, 125 (2000).
 - [6] M. Itakura, J. Phys. Soc. Jpn. **72**, 74 (2003).
 - [7] V. Thanh Ngo and H. T. Diep, J. Appl. Phys. **103**, 07C712 (2008).
 - [8] Y. Nagano, K. Uematsu and H. Kawamura, Phys. Rev. B, **100**, 22 (2019).
 - [9] P. Calabrese, E. V. Orlov, P. Parruccini, and A. I. Sokolov, Phys. Rev. B **67**, 024413 (2003).
 - [10] H. Kawamura and S. Miyashita, J. Phys. Soc. Jpn. **53**, 4138 (1984).
 - [11] M. Wintel, H. U. Everts, and W. Apel, Europhys. Lett. **25**, 711 (1994).
 - [12] W. Stephan and B. W. Southern, Phys. Rev. B **61**, 11514 (2000).
 - [13] M. Caffarel, P. Azaria, B. Delamotte, and D. Mouhanna, Phys. Rev. B **64**, 014412 (2001).
 - [14] P. Azaria, B. Delamotte, F. Delduc, and T. Jolicœur, Nucl. Phys. B **408**, 485 (1993).
 - [15] A. Pelissetto, P. Rossi, and E. Vicari, Phys. Rev. B **63**, 140414 (2001).
 - [16] P. Calabrese, P. Parruccini, and A. I. Sokolov, Phys. Rev. B **66**, 180403 (2002).
 - [17] P. Calabrese, P. Parruccini, A. Pelissetto, and E. Vicari, Phys. Rev. B **70**, 174439 (2004).
 - [18] P. Calabrese and P. Parruccini, Nucl. Phys. B **679**, 568 (2004).
 - [19] G. Zumbach, Phys. Rev. Lett., **71**, 2421 (1993).
 - [20] G. Zumbach, Nucl. Phys. B, **413**, 771 (1994).

- [21] M. Tissier, B. Delamotte, and D. Mouhanna, Phys. Rev. Lett. **84**, 5208 (2000).
- [22] B. Delamotte, M. Dudka, D. Mouhanna, S. Yabunaka, Phys. Rev. B **93**, 064405 (2016).
- [23] Y. Nakayama and T. Ohtsuki. Phys. Rev. D **89**, 126009, (2014).
- [24] Y. Nakayama and T. Ohtsuki. Phys. Rev. D **91**, 021901, (2015).
- [25] G. Tarjus and M. Tissier, Phys. Rev. Lett. **93**, 267008 (2004); M. Tissier and G. Tarjus, Phys. Rev. Lett. **107**, 041601 (2011); L. Canet, H. Chaté, B. Delamotte, and N. Wschebor, Phys. Rev. Lett. **104**, 150601 (2010); L. Canet, H. Chaté, B. Delamotte, and N. Wschebor, Phys. Rev. E **84**, 061128 (2011); L. Canet, H. Chaté, B. Delamotte, and N. Wschebor, Phys. Rev. E **86**, 019904 (2012); O. Coquand, K. Essafi, J. P. Kownacki, and D. Mouhanna, Phys. Rev. E **97**, 030102 (2018); F. Léonard and B. Delamotte, Phys. Rev. Lett. **115**, 200601 (2015); L. Canet, H. Chaté, and B. Delamotte, Phys. Rev. Lett. **92**, 255703 (2004); L. Canet, B. Delamotte, O. Deloubrière, and N. Wschebor, Phys. Rev. Lett. **92**, 195703 (2004).
- [26] J. Henriksson, S. R. Kousvos, and A. Stergiou, SciPost Physics, 9(3), **035** (2020).
- [27] M. Reehorst, S. Rychkov, B. Sirois, B. C. van Rees, arXiv 2405.19411.
- [28] S. El-Showk, M. F. Paulos, D. Poland, S. Rychkov, D. Simmons-Duffin, and A. Vichi Phys. Rev. D **86**, 025022, (2012).
- [29] F. Kos, D. Poland, D. Simmons-Duffin, JHEP **11**, 109, (2014).
- [30] J. Berges, N. Tetradis, and C. Wetterich. Phys. Rep. **363**, 223 (2002).
- [31] C. Wetterich, Nucl. Phys. B **352**, 529 (1991).
- [32] C. Wetterich, Phys. Lett. B **301**, 90 (1993).
- [33] U. Ellwanger, Z. Phys. C **58**, 619 (1993).
- [34] T. R. Morris, Int. J. Mod. Phys. A **9**, 2411 (1994).
- [35] M. Tissier, D. Mouhanna, and B. Delamotte, Phys. Rev. B **61**, 15327 (2000).
- [36] M. Tissier, B. Delamotte, and D. Mouhanna, Int. J. Mod. Phys. A **16**, 2131 (2001).
- [37] M. Tissier, B. Delamotte, and D. Mouhanna, Phys. Rev. B **67**, 134422 (2003).
- [38] D. F. Litim, Nucl. Phys. B **631**, 128 (2002).
- [39] L. Canet, B. Delamotte, D. Mouhanna and J. Vidal, Phys. Rev. D **67**, 065004, (2003).
- [40] L. Canet, B. Delamotte, D. Mouhanna, and J. Vidal, Phys. Rev. B, **68**, 064421 (2003).
- [41] I. Balog, H. Chaté, B. Delamotte, M. Marohnic, and N. Wschebor, Phys. Rev. Lett. **123**, 240604 (2019).
- [42] G. De Polsi and N. Wschebor, Phys. Rev. E, **106** (2), 024111 (2022).

- [43] A. O. Sorokin, arXiv:2205.07199
- [44] M. V. Kompaniets, A. Kudlis, and A. I. Sokolov, Nucl. Phys. B, 950, 114874 (2020).
- [45] D. R. T. Jones, A. Love, and M. A. Moore. J. Phys. C **9**, 743 (1976).
- [46] D. Bailin, A. Love, and M. A. Moore. J. Phys. C **10**, 1159 (1977).
- [47] T. Machado, N. Dupuis, Phys. Rev. E **82**, 041128 (2010).
- [48] L. Canet, H. Chaté, B. Delamotte, Phys. Rev. Lett. **92**, 255703 (2004).
- [49] T. Debelhoir and N. Dupuis, private communication.
- [50] J.-P. Blaizot, R. Mendez-Galain, and N. Wschebor, Phys. Lett. B **632**, 571 (2006).
- [51] J.-P. Blaizot, R. Mendez-Galain, and N. Wschebor, Phys. Rev. E **74**, 051116 (2006).
- [52] J.-P. Blaizot, R. Mendez-Galain, and N. Wschebor, Phys. Rev. E **74**, 051117 (2006).
- [53] S. Yabunaka and B. Delamotte, Phys. Rev. Lett. **119**, 191602 (2017).
- [54] S. Yabunaka and B. Delamotte, Phys. Rev. Lett. **121** 231601 (2018).
- [55] S. Yabunaka and B. Delamotte, Phys. Rev. E **106**, 054105 (2022).
- [56] A. Chlebicki, C. Sánchez-Villalobos, P. Jakubczyk, and N. Wschebor, Phys. Rev. E, **106**, 064135 (2022).
- [57] When a field expansion of the potential is performed, it has been confirmed that the correlation length remains finite around $d = 3$ by integrating the renormalization group flow as shown in [1]. We think that it is interesting to study runaway flows with the current treatment of the full functional dependence of $U_k(\rho, \tau)$ in future studies.
- [58] The resummation plotted here is done without assuming $N_c(d = 2) = 2$